

# Foamability in high viscous non-Newtonian aqueous two-phase systems composed of surfactant and polymer

Ding, Ping; Bakalis, Serafim; Zhang, Zhibing

DOI:

[10.1016/j.colsurfa.2019.123817](https://doi.org/10.1016/j.colsurfa.2019.123817)

License:

Creative Commons: Attribution-NonCommercial-NoDerivs (CC BY-NC-ND)

Document Version

Peer reviewed version

Citation for published version (Harvard):

Ding, P, Bakalis, S & Zhang, Z 2019, 'Foamability in high viscous non-Newtonian aqueous two-phase systems composed of surfactant and polymer', *Colloids and Surfaces A: Physicochemical and Engineering Aspects*, vol. 582, 123817. <https://doi.org/10.1016/j.colsurfa.2019.123817>

[Link to publication on Research at Birmingham portal](#)

## Publisher Rights Statement:

Ping Ding, Serafim Bakalis, Zhibing Zhang, Foamability in high viscous non-Newtonian aqueous two-phase systems composed of surfactant and polymer, *Colloids and Surfaces A: Physicochemical and Engineering Aspects*, 2019, 123817, ISSN 0927-7757.

The version of record can be accessed online at <https://doi.org/10.1016/j.colsurfa.2019.123817> and <http://www.sciencedirect.com/science/article/pii/S0927775719308052>

© The Authors

## General rights

Unless a licence is specified above, all rights (including copyright and moral rights) in this document are retained by the authors and/or the copyright holders. The express permission of the copyright holder must be obtained for any use of this material other than for purposes permitted by law.

- Users may freely distribute the URL that is used to identify this publication.
- Users may download and/or print one copy of the publication from the University of Birmingham research portal for the purpose of private study or non-commercial research.
- User may use extracts from the document in line with the concept of 'fair dealing' under the Copyright, Designs and Patents Act 1988 (?)
- Users may not further distribute the material nor use it for the purposes of commercial gain.

Where a licence is displayed above, please note the terms and conditions of the licence govern your use of this document.

When citing, please reference the published version.

## Take down policy

While the University of Birmingham exercises care and attention in making items available there are rare occasions when an item has been uploaded in error or has been deemed to be commercially or otherwise sensitive.

If you believe that this is the case for this document, please contact [UBIRA@lists.bham.ac.uk](mailto:UBIRA@lists.bham.ac.uk) providing details and we will remove access to the work immediately and investigate.

# Foamability in High Viscous Non-Newtonian Aqueous Two-phase Systems Composed of Surfactant and Polymer

Ping Ding<sup>1</sup>, Serafim Bakalis<sup>2</sup> and Zhibing Zhang<sup>1\*</sup>

<sup>1</sup> School of Chemical Engineering, University of Birmingham, Birmingham B15 2TT, UK

<sup>2</sup> Department of Chemical and Environmental Engineering, University of Nottingham, Nottingham NG7 2RD, UK

\*Corresponding author

## Abstract

Foaming in high viscous and non-Newtonian aqueous phase is generally difficult to be realised. In this work, a surfactant (Sodium Linear Alkylbenzene Sulphonate with alkyl chain lengths varying from C10 to C16) named LAS paste mixed with a co-polymer solution of acrylic acid and maleic acid denoted by Polymer solution was used to generate foam under conditions of sparging without or with agitation, which aims to be used as a coating material of detergent powders. The foam structure/morphology, bubble size, gas holdup and liquid drainage in such surfactant-copolymer system were investigated. It was found that two different types of foam were generated: 1) dispersed spherical air bubbles in highly viscous mixtures of LAS paste and Polymer solution with median size  $d_{50}$  in a range of 20 – 50  $\mu\text{m}$  and gas holdup of 0.20 - 0.44 depending on LAS concentration, 2) bubbles with polyhedral structure in a mixture of LAS paste and Polymer solution diluted with water and size  $d_{50} = 7.0 \pm 0.4$  mm and gas holdup of  $0.93 \pm 0.05$ . The generated foam structures depended on the energy input, air superficial velocity, surfactant concentration and the liquid viscosity. Besides, they even depended on liquid mixing procedures before the foam was generated, resulting from different transfer rates from LAS paste phase to Polymer solution. The comparison of foam behaviours in such complex system and in single-phase liquid was made. For dispersed spherical bubbles, the median size has been



correlated to energy input whilst for bubbles with polyhedral structure the characteristic size has been predicted by considering the balance between their buoyancy and viscous forces generated in the system. Based on the results, the mechanism of foam stabilisation is proposed.

Keywords: Detergent, Foam, Foamability, Foam stabilization, High viscous liquid, Non-Newtonian, Surfactant-copolymer two aqueous phase system.

## I. Introduction

Foams are multiphase colloidal systems, which are formed by trapping gas bubbles in a continuous phase (liquid or solid). They are widely used in food, pharmaceutical, personal care products, flotation and other separation processes, firefighting, petroleum and gas industries [1-3]. Aqueous foam was also used as a carrier of thermoplastic resins to coat carbon fibres [4]. Coating of particles can have a wide range of industrial applications, e.g. to stabilise active ingredient in the particles, to achieve its controlled release, and to improve their flowability. It can often be achieved using a shell material dissolved or dispersed in aqueous phase, which can be pumped through a nozzle to generate tiny liquid droplets and sprayed onto the surface of the core particles in a fluidised bed coater. However, spraying can be difficult when the application requires high viscous liquids as the coating material, and examples include coating of surfactant powders in order to make compact detergent, e.g. detergent with a high concentration of surfactant, which is highly desirable in terms of saving the costs of production and transportation and reducing environmental footprint. The coating aims to improve the flowability of the detergent powders, and storage stability. For such purpose, it is proposed to generate foam from a viscous liquid mixture of LAS and the Polymer so that it can be dispersed by spray due to its much lower specific density than the corresponding liquid, and the foam can potentially be used to coat surfactant powders to make compact detergent. To meet the

objective, it has become essential to investigate the foamability of air in a mixture of highly viscous liquids which are most likely non-Newtonian and may have complex structure.

Foaming of air in a wide range of Newtonian viscous liquids for viscosities up to 6 Pa s has been investigated using rotor-stator mixers [5-7] or nozzles [8]. Foaming of air in a highly viscous shear-thinning liquid in a Kinematica rotor-stator was also reported [9]. All these researches have shown that the foam structure and bubble size strongly depended on the liquid viscosity and processing conditions. Kontziampasis et al [10] have investigated coating particles in a paddle and twin-screw mixer using foams generated in a mixture of starch and whey protein as high viscous fluid. They found that the use of foams generated more effective coating compared to the liquid counterpart. The optimal bubble size was found to be a few millimetres for the coating purpose. However, none of researches has investigated the foam behaviours of air in non-Newtonian liquid mixture made of two immiscible aqueous surfactant and aqueous polymer phases. The mixture differs from normally defined miscible, partially miscible or immiscible systems, and understanding of foaming behaviours in such systems is scientifically important and may help to produce desirable foams for industrial applications.

Regarding their stabilisation, foams are conventionally stabilised by surfactant molecules [11], by aqueous polyelectrolyte/surfactant mixtures or solid particles [12-14]. For the first case, surfactant molecules usually diffuse in water and adsorb at interfaces between air and water. Surfactant molecules tend to orient themselves with their hydrophobic tails sticking out of the surface into the air whereas their heads remain buried in the water. The presence of surfactant molecules at the surface reduces the surface energy and hence the surface tension, and also provides repulsive electrostatic and steric forces to prevent the bubble coalescence. Surface tension is usually at the minimum corresponding to the critical micelle concentration (CMC) of surfactant. Beyond the CMC, the non-dissolved surfactant does not enter the

already saturated gas-liquid interface and instead enters an association with other surfactant molecules in the bulk in a micellar arrangement in which hydrophobic heads come together trying to escape from the water [11]. For foams stabilised by aqueous polyelectrolyte/surfactant mixtures [12], the addition of polyelectrolyte either enhances the overall electrostatic repulsion within the liquid film between gas bubbles or decreases the surface elasticity leading to more densely packed charges at the surface. Solid particles have been incorporated into surfactant-stabilised aqueous foams for many years, but the literature concerned with the ability of particles to act as foam stabilisers in the absence of any other surface-active material is very sparse [13-16]. It is generally expected that the stabilising mechanisms identified in aqueous emulsion films could be relevant to aqueous foam films as well [13]. Depending on the exact system, there are at least two mechanisms by which colloidal particles stabilise foams. In the first case, the particles are required to adsorb at the air-water interface and remain there forming a dense film monolayer or multilayer around the dispersed bubbles impeding coalescence. In the second case, additional stabilisation arises when the particle - particle interactions are such that a three-dimensional network of particles develops in the continuous phase surrounding the bubbles [13].

Yin et al have reported a more complexed foam stabilization mechanism [17]. They have investigated stabilization mechanism of carbon dioxide (CO<sub>2</sub>) foam reinforced by regenerated cellulose (RC) and proposed four stabilization mechanisms as follows. The thickening behaviour of RC in the liquid phase retards the liquid drainage; the RC aggregates adsorb on the interface and liquid enhances the foam stability; the liquid storage effect of RC supplies the thinning liquid film; the liquid film skeleton formed by RC reinforces the foam.

In this study, we have investigated foamability of air in a mixture of surfactant solution (Sodium Linear Alkylbenzene Sulphonate with alkyl chain lengths varying from C10 to C16) named LAS paste and co-polymer solution of acrylic acid and maleic acid denoted by Polymer with different amounts of water under various sparging and agitation conditions. The foamability was characterised in terms of foam structure/morphology, bubble size, gas holdup and liquid drainage. The bubble sizes generated in such systems were predicted by theoretical models. The results were compared with those of foaming in single-phase liquid, and the mechanism of foam stabilization has been proposed.

## **2. Experimental**

### **2.1 Materials and methods**

A concentrated aqueous solution of co-polymer (acrylic acid and maleic acid) that is an industrial precursor (denoted by Polymer) was used with a concentrated aqueous dispersion of surfactant (Sodium Linear Alkylbenzene Sulphonate with alkyl chain lengths varying from C10 to C16) named LAS paste. Both of them were supplied by Procter & Gamble Technical Centres Ltd (Newcastle, UK). According to the supplier, the LAS paste had 46 wt% LAS in water and Polymer had 40 wt% acrylic acid and maleic acid in water. The specific densities of LAS paste and Polymer were  $1000\text{kg/m}^3$  and  $1300\text{kg/m}^3$  respectively.

Viscosities of liquid and foam were measured using a Hybrid Rheometer (Discovery HR-1, TA Instrument) with the geometries of 60 mm and  $2^\circ$  cone, and 40 mm plate with 2 mm gap depending on the materials to be measured. Bubble size and the structures of liquid and foam were measured using optical microscopy and/or stereo microscopy (Olympics, Japan) depending on foam properties. Bubble size distributions were analysed by image analysis using software ImageJ combined with a self-written plugin macro file. The bubble size and

size distribution at each experimental condition were obtained by counting 300-400 bubbles to make sure the results are statically representative.

Surface tension of each liquid was measured by a pendant drop method using a needle of 1 mm (inner diameter) [18, 19]. The images of the pendant drops were monitored using stereo microscopy. The detailed rig description can be found elsewhere [20]. Surface tension of water was first measured at room temperature to test the reliability of the method and the value of  $73 \pm 2$  mN/m was obtained showing a good agreement with the literature report  $72.2 \pm 0.2$  mN/m at  $22^{\circ}\text{C}$  [19]. This validates the reliability of the methodology used here.

## 2.2 Foam generation and characterisation

Foams were generated in a jacketed stirred vessel (diameter  $T = 90$  mm) fitted with a Rushton turbine impeller (diameter  $D = 50$  mm). No baffle was used to avoid the stagnant liquid behind it due to the viscous liquids with yield stress used in this work. Air was sparged by a homemade stainless steel sparger that was a ring - shaped tubing with 8 holes (diameters of tubing and holes were 6 mm (outer diameter) and 1 mm respectively). The selection of Rushton turbine instead of rotor-state mixer was based on the consideration that the relatively large bubbles were aimed to be obtained for particle coating [10].

Two sets of experiments were carried out:

- 1) High viscous liquid: A certain amount of LAS paste was added to Polymer solution in the vessel agitated at 300 rpm for 15 min. After that air was sparged to the mixture to generate foams either by sparging only or sparging combined with agitation at a pre-set speed.
- 2) Less viscous liquid using water dilution: liquids were mixed using two different procedures before air sparging.

- a) Liquid mixing procedure 1: Adding water to LAS paste agitated at 300 rpm for 10 min to obtain a diluted LAS phase. Then it was added to Polymer solution agitated at 300 rpm for 15 min.
- b) Liquid mixing procedure 2: Adding water to Polymer solution at 300 rpm for 10 min to obtain a diluted Polymer solution. Then LAS paste was added to the diluted Polymer solution agitated at 300 rpm for 15 min.

Afterwards air was sparged to the mixture and foams were generated without or with agitation at a pre-set speed.

The gas holdup ( $\epsilon_G$ , volume ratio of gas phase in the foam to the total foam) was calculated by Equation (Eq.)1:

$$\epsilon_G = \frac{H_G - H_L}{H_G} \quad (1)$$

where  $H_G$  is the height of liquid after aeration, and  $H_L$  the initial height of liquid without aeration, which were measured experimentally by placing a ruler close to the vessel and measuring the height of the liquid and resulting foam.

Liquid drainage is defined by the volume of drained liquid after a certain time divided by the initial foam volume (Eq. 2).

$$D = \frac{V_{\text{drained}}}{V_{\text{initial}}} \quad (2)$$

The volume of the drained liquid and the initial foam each was measured by determining its height using a ruler in conjunction with the known stirred tank diameter/cross sectional area.

### 3. Results and discussion

#### 3.1. Foam behaviours and physical properties

##### 3.1.1 Morphology and structure

The structures of LAS paste and a mixture of 20 wt% LAS paste/80wt% Polymer solution are shown in Fig. 1. As can be seen, LAS paste is a two-phase system with dispersed aggregates that consist of small particles of 1-2  $\mu\text{m}$  in diameter (Fig. 1(a)). These small particles might be LAS micelles and lamella due to the high LAS concentration in initial LAS paste ( $\sim 46$  wt%) [21]. This assumption was consistent with the fact that after adding water to LAS paste in a weight ratio of 1:1, the aggregates and particles were dissolved and the diluted LAS liquid became single clear phase. Further characterization of the particles/aggregates is beyond the scope of this work. The mixture of 20 wt% LAS paste/80wt% Polymer shows a two-phase system with aggregates (LAS) dispersed in Polymer solution (Figure 1(b)). It was observed that the LAS paste and Polymer solution when mixed formed two separate phases. At a LAS paste concentration as low as 0.5 g/L, the liquid was still turbid. In other words, the CMC of LAS in Polymer solution should be lower than 0.5g/L. This is in contrast to a CMC of 0.65 g/L for the commercial  $\text{C}_{10-13}$  LAS in water as reported by Smulders [22]. This difference may be explained by the observed water transfer from LAS phase to Polymer phase leading to the increase of local LAS concentration and the formation of particles/aggregates. Clearly, this complex mixture differs from normally defined miscible, partially miscible or immiscible liquid systems. This water transport phenomenon between phases will be discussed in details with experimental validation in Appendix.

Fig. 1 here

### 3.1.2 Viscosity

The viscosity of LAS paste shows viscous non-Newtonian shear thinning behaviour (data not shown) which is consistent with its two-phase structure (see Fig. 1(a)). The Polymer solution was a viscous Newtonian liquid with viscosity up to 4.7 Pa s (the dotted line in Fig. 2(a)). Addition of LAS paste to a final concentration of 3 wt% had practically no effect on the mixture viscosity. With the further increase of LAS paste concentration, the mixtures showed shear thinning behaviour. At 30wt% LAS paste and low shear rate range ( $< 2 \text{ s}^{-1}$ ), the mixture viscosity is higher than Polymer solution due to the high viscous effect of LAS paste ( $\sim 16 \text{ Pa} \cdot \text{s}$  at a shear rate of  $1 \text{ s}^{-1}$ ). Addition of water significantly decreased the mixture viscosity (Fig. 2(b)). These shear thinning viscosity data can be well modelled using Herschel-Bulkley equation (Eq. 3) [23] as shown in Fig. 2 where the lines represent the model fitting results.

(3)

— ———

(3a)

where  $\tau$  is the shear stress,  $\tau_o$  is yield stress,  $k$  consistency constant,  $\dot{\gamma}$  shear rate,  $n$  rate index and  $\eta$  dynamic viscosity.

Fig. 2 here

### 3.1.3 Surface tension

The surface tensions of different mixtures are summarized in Fig. 3. The surface tension of Polymer solution was  $95 \pm 2 \text{ mN/m}$  indicating it may be difficult for air to foam in it. The

surface tension of LAS paste was  $34.6 \pm 0.4$  mN/m, which is broadly in line with the literature data of 29.3-31.8 mN/m ( $C_{11}$ - $C_{13}$ ) [24]. The surface tension of the mixtures was around 65 mN/m when LAS concentration varies from 3 - 30 wt% and the amount of water added was up to 25 wt%. At a higher water amount 50 wt%, the surface tension of the mixture reduced to  $\sim 35$  mN/m which is close to that of LAS paste. The results show that the addition of LAS paste to Polymer solution reduced the surface tension of the mixture and might make it suitable for the surfactant to stabilise foam. In general, for accurate measurement of surface tension, samples should be measured before, during and after each experiment, as small levels of contamination may dramatically change the surface tension. We measured surface tension of the liquids soon after the drainage and 3 months after the experiments, which were used to determine the error bars of the data. The results are repeatable showing the good storage stability of both LAS paste and Polymer solution as indicated by the small error bars in Fig 3. However, during and immediate after experiments it was not possible to measure the liquid surface tension due to presence of the foams in the liquid.

Fig. 3 here

### 3.2. Foaming in highly viscous liquid

#### 3.2.1. Foaming by sparging without and with agitation

The first set of foaming experiments was carried out using a mixture of LAS paste and Polymer without dilution. The typical foaming results are shown in Fig. 4. After air was sparged without agitation, the foams were initially generated at the top of liquid and the volume of the liquid started to increase due to gas holdup. After 30 min sparging, no further

increase of gas holdup with time was found (data not shown). Therefore the foaming was considered to reach a steady state. Clearly the resulting foams were non-uniform and the bubble sizes on average decreased from the top to bottom in the vessel. The median bubble size ( $d_{50}$ ) was approximately 3 mm in the top part of the foams (around 40 vol%) and 36  $\mu\text{m}$  in the bottom part. The gas holdup was  $0.44 \pm 0.02$ . At an impeller speed of 300 rpm the resulting foams were relatively uniform spatially with  $d_{50} = 43 \mu\text{m}$ ,  $\text{Span} = (d_{90}-d_{10})/d_{50} = 1.9$  and gas holdup =  $0.41 \pm 0.03$  (Fig. 4(b)), where,  $d_{10}$ ,  $d_{50}$  and  $d_{90}$  represent 10%, 50% and 90% (number percent) of bubbles with diameters below those values. Clearly, for the highly viscous shear thinning mixtures it is necessary to use agitation during sparging to disperse air bubbles in liquid and generate foams with uniform bubble size that are distributed homogeneously. The typical structure of foams generated under agitation is shown in Fig. 4(c) and 4(d). The results indicate that the foams consisted of three phases: air bubbles, LAS aggregates and liquid Polymer. Here, LAS aggregates filled the gaps between bubbles through the aggregates network (Fig. 4(d)).

Fig. 4 here

### 3.2.2 Effect of LAS concentration

The effect of LAS concentration on foaming results is shown in Fig. 5. The median bubble size ( $d_{50}$ ) initially increased from 20 - 30  $\mu\text{m}$  to 30 – 50  $\mu\text{m}$  depending on the gas flow rate when LAS paste concentration increased from 3 wt% to 10 wt% and then maintained nearly constant up to 40 wt% LAS paste (Fig. 5(a)).

Gas holdup as a function of LAS paste concentration at different gas superficial velocities is shown in Fig. 5(b). The results indicate that the gas holdup initially increased with the increase of LAS concentration from 3 wt% to 10 wt% and then maintained practically constant to 20 wt%. After that the gas holdup decreased at the higher LAS paste concentration of 40 wt%. These phenomena were observed at the all gas superficial velocities from 1.0 mm/s to 2.6 mm/s, the reason for which will be discussed later. In other words, relatively higher gas holdup was obtained at LAS paste concentration of 10-20 wt%.

The liquid drainage after 24h significantly decreased from 0.6 to 0.04 with the increase of LAS paste concentration from 3 wt% to 20 wt% and then decreased slowly to almost zero at LAS concentration of 40 wt% (Fig. 5(c)).

These results showed that the desirable LAS concentration was 20 wt% where the generated foams were associated with big bubble size, high gas holdup and relatively low liquid drainage. Further increasing LAS paste concentration to 40 wt% led to a significant increase of liquid yield stress (0 Pa at 3 and 10 wt%, 0.90 Pa at 20 wt % and 3.5 Pa at 40 wt%). In highly viscous liquid, agitation tends to cause cavern formation, regions of liquid mixing and motion around the impeller, outside of which the fluid is stagnant or nearly so. Even inside the cavern, mixing is slow. The cavern size is proportional to the reciprocal value of liquid yield stress [25]. This might imply that the increased yield stress at higher LAS concentration (i.e. 40 wt%) could lead to the worse mixing and foaming performances.

Fig. 5 here

### 3.2.3 Effect of energy input

The evolution of median diameter (or any other mean diameter) during de-aggregation/breakage process of particles/drops/bubbles may be described in terms of processing time and energy dissipation rate or in terms of energy density (product of energy dissipation rate and processing time) by so called size-energy models [7, 26-28]. When the systems reaches the equilibrium where the size no longer changes with time, median diameter may be described in terms of average energy dissipation rate ( :

(4)

$$\bar{\varepsilon} = \frac{P_0 N^3 D^5}{V} \quad (5)$$

where  $a$  and  $b$  are proportionality constants,  $P_0$  is power number,  $N$  impeller speed,  $D$  impeller diameter and  $V$  is volume of the liquid. Power number  $P_0$  is a function of Reynolds number ( $Re$ ) for laminar flow that can be calculated from Eq. 6.

$$\text{---} \quad (6)$$

where the dynamic viscosity of the mixture ( ) under a certain shear rate range was determined from the viscosity measurement. The average shear rate ( in the stirred vessel with a Rushton turbine is give by Harnby et al. [29]:

(7)

The  $Re$  number in high viscous liquid at the investigated impeller speeds was less than 15. According to Nienow et al. [30], at low Reynolds number ( $Re < 50$ ), power number in gassed system is the same as that in ungassed mixtures. Therefore, the ungassed power number

without baffles can be obtained from the previous report [31].

The size-energy model (Eq. 4) has been reported in literature to successfully describe the grinding of solid particles where  $b$  in the range of 0.68 – 0.72 was obtained [26, 32]. It has also been adopted to correlate average droplet size with energy input during liquid/liquid emulsification using different types of high shear mixers and in such cases  $b$  of 0.4 was reported [27, 28]. For the relation between the bubble size and energy input, the same energy-size model can be applied [11, 33]. Plotting our experimental  $d_{50}$  as a function of energy dissipation rate (Eq. 4) in log-log coordinates, all data points can be collapsed into a straight line (Fig. 6) with constant  $a = 44.9 \mu\text{m}$ , slope  $b = 0.37$  and coefficient of determination  $r^2 = 0.98$ , which indicates that the relation between the bubble size and energy input can be described by this model well. It seems that  $b = 0.37$  is similar to the liquid/liquid dispersion value ( $b = 0.4$ ) instead of solid/liquid dispersion ( $b = 0.7$ ). These results indicate that the relation between bubble size and energy input in this two-phase liquid with complex structures is similar to that for single-phase liquid.

Fig. 6 here

### 3.3. Foaming in less viscous liquid

The second set of foaming experiments was carried out using less viscous liquid by water dilution of LAS paste and Polymer mixture, which reduced their viscosities to less than 1 Pa s (see Fig 1(b)). The foaming experiments were also undertaken under sparging without and with agitation respectively.

#### 3.3.1 Foaming without agitation

The results of foaming in less viscous liquid with sparging only are summarized in Fig. 7. Fig. 7(a) shows the foam generated using liquid mixing procedure 1: LAS paste was first mixed with water to form diluted LAS phase and then it was mixed with Polymer solution. It was observed that the foams initially generated at the top of the liquid had the polyhedral structure arranged in a spatially periodic manner. With time evolution the height of the liquid was reduced and eventually all the liquid was foamed producing the same foam structure. This structure is common for foams [11] but different from those generated in the highly viscous liquid where spherical bubbles of 20 - 50  $\mu\text{m}$  were dispersed in liquid phase (Fig. 5(c) and 5(d)). The bubble size distribution is quite uniform with  $d_{50} = 7.0 \text{ mm}$ , and  $\text{Span} = (d_{90}-d_{10})/d_{50}=0.48$ . Initial gas holdup was estimated as  $0.93\pm0.05$ . The results indicate the foams generated under this condition may be desirable for particle coating [10]. Davidson and Schuler [34] studied bubble formation in liquids under sparging without agitation and obtained the following theoretical expression to determine bubble diameter ( $d$ ) based on a balance between buoyancy and viscous forces (Equation 8)

$$\text{---} \quad (8)$$

where  $Q$  is gas flow rate per orifice ( $\text{m}^3/\text{s}$ ) and  $g$  is the gravitational acceleration. They concluded that this relation was valid for an orifice diameter of  $6.68 \times 10^{-4} \text{ m}$ , liquid viscosity ( ) ranging from 0.5 to 1.05 Pa.s, and gas flow rate ranging from 0 to  $2.5 \times 10^{-6} \text{ m}^3/\text{s}$ . Ramakrishnan et al. [35] also studied the effect of viscosity on bubble formation both theoretically and experimentally, finding Equation 8 is applicable to a range of gas flow rates 0 to  $6 \times 10^{-5} \text{ m}^3/\text{s}$ , orifice diameters 0.0037 to 0.007 m, and viscosities 0.04 to 0.5 Pa.s. Corresponding to experimental conditions in this work, the orifice diameter was 0.001 m, viscosity nearly 1 Pa s, and air flow rate  $6.25 \times 10^{-7} \text{ m}^3/\text{s}$ , which are well in the range of

above conditions. The calculated bubble size using Equation 8 is 0.0063 m, which is in a good agreement with the measured  $d_{50}$  value of 0.007 m. Again, these results indicate that the relation between bubble size in this two- phase liquid with complex structures can be estimated based on Equation (8) for single-phase liquid.

When foaming in less viscous liquid using liquid mixing procedure 2, i.e. mixing Polymer solution and water first to form diluted Polymer phase and then adding LAS paste, the results (Fig. 7(b) & 7(c)) were significantly different from those obtained when using liquid mixing procedure 1. After air sparging, the structure of foams initially generated on the top of liquid looked similar to that shown in Fig. 7(a) (image not shown). However, after 10 min sparging the foam structure became less uniform and the phase separation between LAS phase and Polymer phase in the liquid was observed (Fig. 7(b) and 7(c)).

From the characterization of physical properties in Section 3.1 and the results in Appendix, we know that: 1) either LAS paste or Polymer was miscible with water but they were immiscible with each other, 2) water showed transfer from LAS phase to Polymer phase. In the liquid produced by mixing procedure 1, 180 ml LAS paste phase (80 g LAS paste + 100g water) was dispersed in 169 ml Polymer phase (220g) resulting in initial LAS phase volume fraction of 51.5 vol%. In mixing procedure 2, 80 ml LAS paste (80g) was dispersed in 269 ml Polymer phase (100g water + 220g Polymer solution) resulting in initial LAS phase volume fraction of 22.9 vol%. We observed water transfer from diluted LAS phase (no aggregates) to Polymer phase, leading to the formation of the aggregates in LAS phase close to the interface of LAS and Polymer phases with time (see Appendix). However, the water transfer was not instantaneous, and might not be completed during the foaming process. Therefore, the water content in LAS phase was higher using procedure 1 than 2. At the volume fraction of dispersed phase around 51.5%, phase inversion or multiphase dispersion could occur at

aqueous-aqueous two phase systems [36]. The different foaming results between two liquid mixing procedures might be explained by the different initial volume fractions of dispersed LAS phase. Specifically, when the initial volume fraction of LAS phase was 51.5 vol%, uniform foam was generated, which resulted from that LAS phase might form continuous networks and Polymer phase might be dispersed. For liquid produced by mixing procedure 2, the volume fraction of LAS phase was only 22.9%, which might form fragmented networks in the dispersed phase.

Liquid drainages were 0.4 and 0.53 after 24h when using two liquid mixing procedures respectively, which indicates that the foams generated using procedure 1 were more significant than that generated using procedure 2. This further shows the effect of liquid mixing procedures on the foaming results.

Considering the foam structure shown in Fig. 4 and the discussion above, a foam stabilization mechanism is proposed: the LAS and Polymer phases are immiscible with each other but water tends to transfer from LAS phase to Polymer phase resulting in the increase of local LAS concentration, and consequently the formation of particles/aggregates. The transferred water from LAS phase is then miscible with Polymer phase. In other words, LAS phase with aggregates is dispersed in Polymer phase under agitation conditions. These LAS aggregates may form three-dimensional networks in Polymer phase, which traps the base liquid surrounding the bubbles, see Fig 4(d). The foams are then stabilised by the dissolved surfactant and these aggregate networks. For an initial volume fraction of LAS phase of 25 vol% (20 wt%) in high viscous LAS paste/Polymer mixture, the bubbles generated might be stabilised by both the dissolved surfactant and the fragmented networks of LAS. Moreover, the high viscous liquid reduces the liquid film drainage rate, and then enhances the foam stability. When the diluted LAS paste with an initial volume fraction of 51.5 vol% (20wt% LAS and 25wt% water) was mixed Polymer solution, the multiple phase/phase inversion

might occur [35]. In this case, Polymer phase might be dispersed and LAS phase might form continuous networks, which with the dissolved surfactant stabilise bubbles in the generated forms.

Fig. 7 here

### 3.3.2 Foaming with agitation

The results of foaming in less viscous liquid using sparging with agitation for liquid mixing procedure 1 are summarized in Fig. 8. At 300 rpm, foams initially generated from the top of the liquid showed a structure similar to that in Fig. 7(a) and the median bubble size  $d_{50}$  was 6.1 mm. However, the bottom foams showed spherical bubbles in the liquid phase with  $d_{50}$  of 40  $\mu\text{m}$ . Increasing impeller speed from 300 rpm to 600 rpm, the foams became visually uniform spatially with spherical bubbles of  $d_{50} = 46 \mu\text{m}$  as shown in Fig. 8(a). The effect of water content on bubble size is shown in Fig. 8(b). It shows that the bubble size increases with water content. In other words, bubble size increases as liquid viscosity decreases. Fig. 8(c) clearly shows that the liquid drainage after 24 h increases with the water content. The gas hold-up in this case was  $0.67 \pm 0.04$ .

Fig. 8 here

### 3.3.3 Viscosity of foam

The viscosities of liquid and the resulting foam are shown in Fig. 9. It is interesting to notice that the foam viscosity is higher than that of initial liquid in both high viscous liquid and less viscous liquid (under the condition of sparging with agitation). This might be explained by

the increased gas surface area and energy after foaming. Once foam was generated the total surface area of bubbles in liquid significantly increased leading to the increased surface energy and therefore the foam viscosity.

It should be indicated that the aim of this study was to generate foams in high viscous non-Newtonian liquid for particle coating, which requires the foams to be pumped easily. Although the viscosity of the generated forms is higher in comparison with the initial liquid, their specific density can be considered to have been significantly reduced. Consequently, the resistance of the foams to flow may be reduced, which remains to be validated in future work.

Fig. 9 here

#### **4. Conclusions**

Aqueous LAS and aqueous Polymer phases are immiscible with each other but water tends to transfer from the LAS phase to Polymer phase resulting in the increase of the local LAS concentration and consequently the formation of particles/aggregates. As a result, a mixture of LAS paste and Polymer phase showed a two-phase structure with the surfactant of LAS paste dispersed as the aggregates consisting of small particles of 1 - 2  $\mu\text{m}$ . The foaming results depended on the concentrations of LAS paste and Polymer phase in the system, processing conditions and liquid mixing procedures before the forms were generated, which determined the initial volume fraction of the two phases.

For high viscous liquid with viscosity up to 5 Pa. s, the generated foam structure is characterised by the dispersed spherical bubbles in base fluid with size  $d_{50}$  in the range of 20 - 50  $\mu\text{m}$  and gas holdup 0.20 - 0.44 depending on LAS concentration. The relation between

the bubble size and energy input can be described by the size – energy equation (Equation 4) with  $b = 0.37$ , which is similar to the results of foaming in single-phase liquid.

When foaming in less viscous liquid using water dilution, two foam structures were generated with the desirable initial volume fraction of LAS phase (51.5 vol%), which was identified based on liquid mixing procedure 1. With agitation at 600 rpm, the generated foam structure was spatially uniform, similar to that in high viscous liquid. However, without agitation, the generated foams had a polyhedral structure with bubble size  $d_{50} = 7.0 \pm 0.4$  mm and gas holdup  $0.93 \pm 0.05$ . The foams might be desirable for particle coating. The bubble size in this case can be predicted using Equation 8, similar to the results of foaming in single-phase liquid.

Based on the experimental results, a new foam stabilization mechanism has been proposed, i.e. when foaming in a mixture of LAS paste and Polymer solution, the bubbles were surrounded by Polymer and possible dissolved surfactant molecules trapped in LAS aggregates which formed fragmented or continuous three-dimensional networks in the base liquid, depending on the initial volume fraction of LAS paste.

## **Acknowledgments**

This work was supported by the Department for Business Innovation and Skills, and the government's Advanced Manufacturing Supply Chain Initiative (AMSCI), UK via the project CHARIOT.

## **Nomenclature**

a, b – Constants defined in Equation 6

d – Bubble diameter [m]

$d_{10}$ ,  $d_{50}$  and  $d_{90}$  – 10%, 50% and 90% (number) of bubbles with diameters below those values [m]

$g$  – Gravitational acceleration [ $\text{m/s}^2$ ]

$H_L$  – The height of unaerated liquid [m]

$H_G$  – The height of aerated liquid [m]

$k$ ,  $n$  – constants with units  $\text{Pa s}^n$  and [-] respectively defined in Equation 3

$N$  – Impeller speed [1/s]

$P_0$  – Power number

$Q$  – Gas flow rate per orifice [ $\text{m}^3/\text{s}$ ]

$t$  – Time [s]

Greek Letters

$\epsilon$  – Mean energy dissipation rate [ $\text{W/kg}$ ]

$\alpha$  – Gas holdup [-]

$\dot{\gamma}$  – Shear rate [1/s]

$\eta$  – Viscosity [ $\text{Pa s}$ ]

$\rho_L$  – Liquid density [ $\text{kg/m}^3$ ]

$\tau$  – Shear stress [Pa]

$\tau_0$  – Yield stress [Pa]

## References

- [1] O. Arjmandi-Tash, A. Trybala, F.M. Mandi, N.M. Kovalchuk, V. Starov, Foams built up by non-Newtonian polymeric solutions: Free drainage, Colloids Surf., A, 521 (2017) 112-120.
- [2] S. Farrokhpay, The significance of froth stability in mineral flotation - A review, Adv. Colloid Interface Sci., 166 (2011) 1-7.

- [3] A. Arzhavitina, H. Steckel, Foams for pharmaceutical and cosmetic application, *Int. J. Pharm.*, 394 (2010) 1-17.
- [4] R.R. Chary, D.E. Hirt, Coating carbon-fibers with a thermoplastic polyimide using aqueous foam, *Polym. Compos.*, 15 (1994) 306-311.
- [5] W. Hanselmann, E. Windhab, Flow characteristics and modelling of foam generation in a continuous rotor/stator mixer, *J. Food Eng.*, 38 (1998) 393-405.
- [6] A.B.J. Kroezen, J.G. Wassink, E. Bertlein, Foam generation in a rotor stator mixer, *Chem. Eng. Process.*, 24 (1988) 145-156.
- [7] C. Balerin, P. Aymard, F. Ducept, S. Vaslin, G. Cuvelier, Effect of formulation and processing factors on the properties of liquid food foams, *J. Food Eng.*, 78 (2007) 802-809.
- [8] T. Maxworthy, C. Gnann, M. Kurten, F. Durst, Experiments on the rise of air bubbles in clean viscous liquids, *J. Fluid Mech.*, 321 (1996) 421-441.
- [9] N. Muller-Fischer, E.J. Windhab, Influence of process parameters on microstructure of food foam whipped in a rotor-stator device within a wide static pressure range, *Colloids Surf., A*, 263 (2005) 353-362.
- [10] D.M. Kontziampasis, J. Mohammed, J. Castro, D. W. York, Coating particles using high viscous fluids and foams with non-ideal mixers, *ChemEngDayUK*, Birmingham, 27-28, March, (2017).
- [11] R.C. Darton, K.H. Sun, The effect of surfactant on foam and froth properties, *Chem. Eng. Res. Des.*, 77 (1999) 535-542.
- [12] N. Kristen, R. von Klitzing, Effect of polyelectrolyte/surfactant combinations on the stability of foam films, *Soft Matter*, 6 (2010) 849-861.
- [13] T.S. Horozov, Foams and foam films stabilised by solid particles, *Curr. Opin. Colloid Interface Sci.*, 13 (2008) 134-140.

- [14] B.P. Binks, Particles as surfactants - similarities and differences, *Curr. Opin. Colloid Interface Sci.*, 7 (2002) 21-41.
- [15] A.C. Martinez, E. Rio, G. Delon, A. Saint-Jalmes, D. Langevin, B.P. Binks, On the origin of the remarkable stability of aqueous foams stabilised by nanoparticles: link with microscopic surface properties, *Soft Matter*, 4 (2008) 1531-1535.
- [16] U.T. Gonzenbach, A.R. Studart, E. Tervoort, L.J. Gauckler, Stabilization of foams with inorganic colloidal particles, *Langmuir*, 22 (2006) 10983-10988.
- [17] X. Yin, W.L. Kang, S.Y. Song, Z.T. Huang, X.Y. Hou, H.B. Yang, Stabilization mechanism of CO<sub>2</sub> foam reinforced by regenerated cellulose, *Colloids Surf., A*, 555 (2018) 754-764.
- [18] J.P. Garandet, B. Vinet, P. Gros, Considerations on the pendant drop method - a new look at Tate law and Harkins correction factor, *J. Colloid Interface Sci.*, 165 (1994) 351-354.
- [19] J.D. Berry, M.J. Neeson, R.R. Dagastine, D.Y.C. Chan, R.F. Tabor, Measurement of surface and interfacial tension using pendant drop tensiometry, *J. Colloid Interface Sci.*, 454 (2015) 226-237.
- [20] P. Ding, B. Wolf, W.J. Frith, A.H. Clark, I.T. Norton, A.W. Pacek, Interfacial tension in phase-separated gelatin/dextran aqueous mixtures, *J. Colloid Interface Sci.*, 253 (2002) 367-376.
- [21] J. A. Stewart, A. Saiani, A. Bayly, G. J. T. Tiddy, *Colloids Surf., A*, 338 (2009) 155-161.
- [22] E. Smulders, *Laundry Detergents*, Wiley-VCH Verlag, Weinheim (2002) p.55.
- [23] H.A. Barnes, *A Handbook of Elementary Rheology*, The University of Wales, Institute of Non-Newtonian Fluid Mechanics, UK, (2000).
- [24] D.L. Smith, Impact of composition on the performance of sodium linear alkylbenzenesulfonate (NaLAS), *J. Am. Oil Chem. Soc.*, 74 (1997) 837-845.

- [25] A. Amanullah, S.A. Hjorth, A.W. Nienow, A new mathematical model to predict cavern diameters in highly shear thinning, power law liquids using axial flow impellers, *Chem. Eng. Sci.*, 53 (1998) 455-469.
- [26] M.W. Gao, E. Forssberg, Prediction of product size distributions for a stirred ball mill, *Powder Technol.*, 84 (1995) 101-106.
- [27] H. Karbstein, H. Schubert, Developments in the continuous mechanical production of oil-in-water macro-emulsions, *Chem. Eng. Process.*, 34 (1995) 205-211. [28] A.W. Pacek, P. Ding, A.T. Utomo, Effect of energy density, pH and temperature on de-aggregation in nano-particles/water suspensions in high shear mixer, *Powder Technol.*, 173 (2007) 203-210.
- [29] N. Harnby, M.H. Edwards, A.W. Nienow, *Mixing in the Process Industries*, 2nd ed, (2000).
- [30] A.W. Nienow, D.J. Wisdom, J. Solomon, V. Machon, J. Vlcek, The effect of rheological complexities on power-consumption in an aerated, agitated vessel, *Chem. Eng. Commun.*, 19 (1983) 273-293.
- [31] J.R. Couper, W.R. Penney, J.R. Fair, S.M. Walas *Chemical Process Equipment: Selection and Design*, Chapter 10 Mixing and Agitation, Third Edition (2010).
- [32] S. Mende, F. Stenger, W. Peukert, J. Schwedes, Mechanical production and stabilization of submicron particles in stirred media mills, *Powder Technol.*, 132 (2003) 64-73.
- [33] N. Muller-Fischer, D. Suppiger, E.J. Windhab, Impact of static pressure and volumetric energy input on the microstructure of food foam whipped in a rotor-stator device, *J. Food Eng.*, 80 (2007) 306-316.
- [34] J.F. Davidson, and B. O. G. Schuler, Bubble formation at an orifice in a viscous liquid, *Chem. Eng. Res. Des.*, 75 (1997) S105-S115.
- [35] S. Ramakrishnan, R. Kumar, N.R. Kuloor, Studies in bubble formation - I. bubble formation under constant flow conditions, *Chem. Eng. Sci.*, 24 (1969) 731-747.

[36] A.W. Pacek, P. Ding, A.W. Nienow, The effect of volume fraction and impeller speed on the structure and drop size in aqueous/aqueous dispersions, *Chem. Eng. Sci.*, 56 (2001) 3247-3255.

### Figure Captions:

Fig. 1 Optical images showing structure of (a) LAS paste and (b) 20 wt% LAS paste/80wt% Polymer solution.

Fig. 2 Viscosities of (a) the mixtures of LAS paste and Polymer solution (●) 3 wt% LAS paste, (○) 10 wt% LAS paste, (▼) 20 wt% LAS paste, (Δ) 30wt% LAS paste, (b) the less viscous liquid of LAS paste, Polymer solution and water, (●) 20 wt% LAS paste/25 wt% water/55 wt% Polymer solution, (○) 20 wt% LAS paste/35 wt% water/45 wt% Polymer solution, (▼) 10 wt% LAS paste/40 wt% water/50 wt% Polymer solution. Lines are from the model fitting by Eq. (3a).

Fig. 3 (a) Effect of LAS paste concentration on the surface tension of LAS paste and Polymer solution mixtures, (b) Effect of additional water amount on the surface tension of (●) LAS paste, (▼) Polymer solution, (■) mixture with 10 wt% LAS paste, (□) mixture with 20 wt% LAS paste.

Fig. 4 Foams generated at 20 wt% LAS paste/80 wt% Polymer solution and air superficial velocity of 1.3 mm/s: (a) sparging only, (b) impeller speed of 300 rpm, (c) and (d) structures at different scales for the system at condition (b).

Fig. 5 Effect of LAS paste concentration on (a) bubble size at air superficial velocity: (●) 0.5 mm/s, (○) 1.3 mm/s, (▼) 2.6 mm/s; (b) gas holdup at superficial velocity: (●) 1.3 mm/s, (○) 2.0 mm/s, (▼) 2.6 mm/s : and (c) drainage after 24 h at air superficial velocity 2.6 mm/s, 300 rpm. The maximum relative error of  $d_{50}$  from repeated experiments is 7%, and that of gas holdup and drainage is 4%.

Fig. 6 Effect of energy dissipation rate on bubble size at 20 wt% LAS paste/80 wt% EW and air superficial velocity 2.6 mm/s.

Fig. 7 Foaming in less viscous liquid: 25% water, 20% LAS paste and 55 wt% Polymer solution at air superficial velocity 0.8 mm/s without agitation using (a) liquid mixing procedure 1 and (b) & (c) liquid mixing procedure 2.

Fig. 8 Foaming in less viscous liquid with agitation at 20wt% LAS paste with varying Polymer solution, 600 rpm and air superficial velocity 1.3 mm/s, (a) foam structure at 25 wt% water; (b) bubble size and (c) drainage after 24 h as a function of water concentration. The straight line only indicates the trend.

Fig. 9 Viscosities of initial liquid mixture and foam at (a) 20wt% LAS paste/80 wt% Polymer solution, 300 rpm, and air superficial velocity 2.6 mm/s; (b) 20wt% LAS paste/55 wt% Polymer solution/25 wt% water, 600 rpm, and air superficial velocity 2.6 mm/s, (●) liquid, (○) foam.

## **Appendix - Water Transfer between LAS Paste and Polymer Phases**

Water transfer between Polymer and LAS paste phases was estimated in bottles using two liquid mixing procedures (see Section 2.2.). In the liquid produced by mixing procedure 1, 67.7 ml Polymer solution was placed in a bottle. 32 ml LAS paste was mixed with 40 ml water forming 72 ml diluted LAS paste phase, which was then placed on the top of Polymer solution as shown in Fig. A1a (left). In the liquid produced by mixing procedure 2, 67.7 ml Polymer was mixed with 40 ml water forming 107.7 ml diluted Polymer phase, on which 32 ml LAS paste was then placed as shown in Fig A1a (right).

In these two cases the overall volume fractions of the Polymer, LAS paste and water were exactly the same but the initial volume fraction of LAS phase was 51.5 vol% in mixing procedure 1 and 22.9 vol% in mixing procedure 2 respectively. This volume difference can be clearly seen in Fig. A1a.

The LAS paste phase was a cloudy two-phase system showing dispersed aggregates (Fig. A1a (right)). After the dilution, the aggregates disappeared, resulting in one clear phase (Fig. A1a (left)). Once the diluted LAS paste and Polymer phases were contacted, the interphase appeared indicating: 1) the two phases were not miscible with each other; 2) the water migrated from top LAS paste phase to bottom Polymer phase, resulting in the increase of the local LAS concentration in the top phase and consequently the formation of aggregates (cloudy interphase). For mixing procedure 1, as time evolved, the water continuously transferred from LAS paste phase to Polymer phase leading to the reduction of the volume of the LAS paste phase. After 180 days, the volume fraction of LAS paste phase reduced to 32.5 vol%, which is close to the initial LAS volume fraction 22.9 vol%. For the mixing procedure 2, the volume reduction of the LAS paste phase was not significant, indicating very slow water transfer from the LAS paste phase to Polymer phase if any. This might be explained by that the initial LAS paste contained 46 wt% LAS (from the supplier) that formed compact

aggregates consisting of 1-2  $\mu\text{m}$  small particles. These aggregates could trap water inside and slow down/prohibit the water transfer at the interphase of LAS paste and Polymer phases.

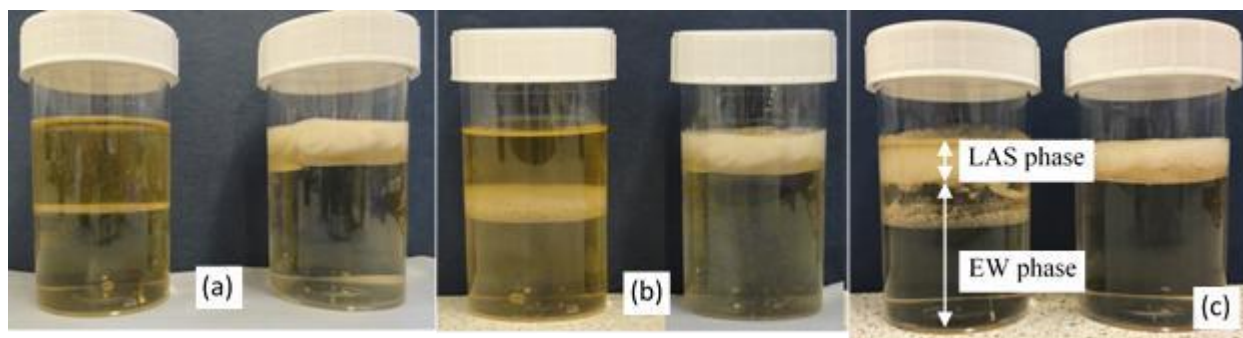


Fig. A1. Images of water transfer behaviour between LAS paste and Polymer solution phases at different time: (a) 0 min, (b) 6 days, (c) 180 days, left – mixing procedure 1 and right - mixing procedure 2.

The water transfer rate was estimated using image analysis (ImageJ). The volume of LAS paste phase as a function of time is plotted in Fig. A2. As can be seen, before 1000 h all data can be practically fitted using a straight line with the slope 0.0263 ml/h ( $R^2 = 0.904$ ), which is the water transfer rate from LAS paste phase to Polymer phase. Considering the interphase area between Polymer and LAS paste phases ( $0.0021 \text{ m}^2$ ) the water transfer rate can be estimated as  $0.207 \text{ g/m}^2 \text{ min}$ .

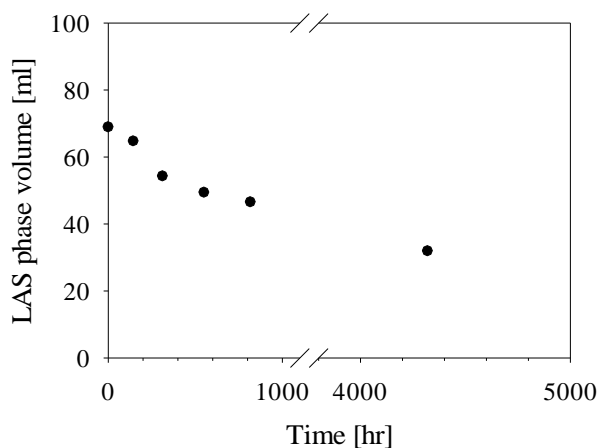


Fig. A2. The volume of LAS paste phase as a function of storage time.

Figure 1

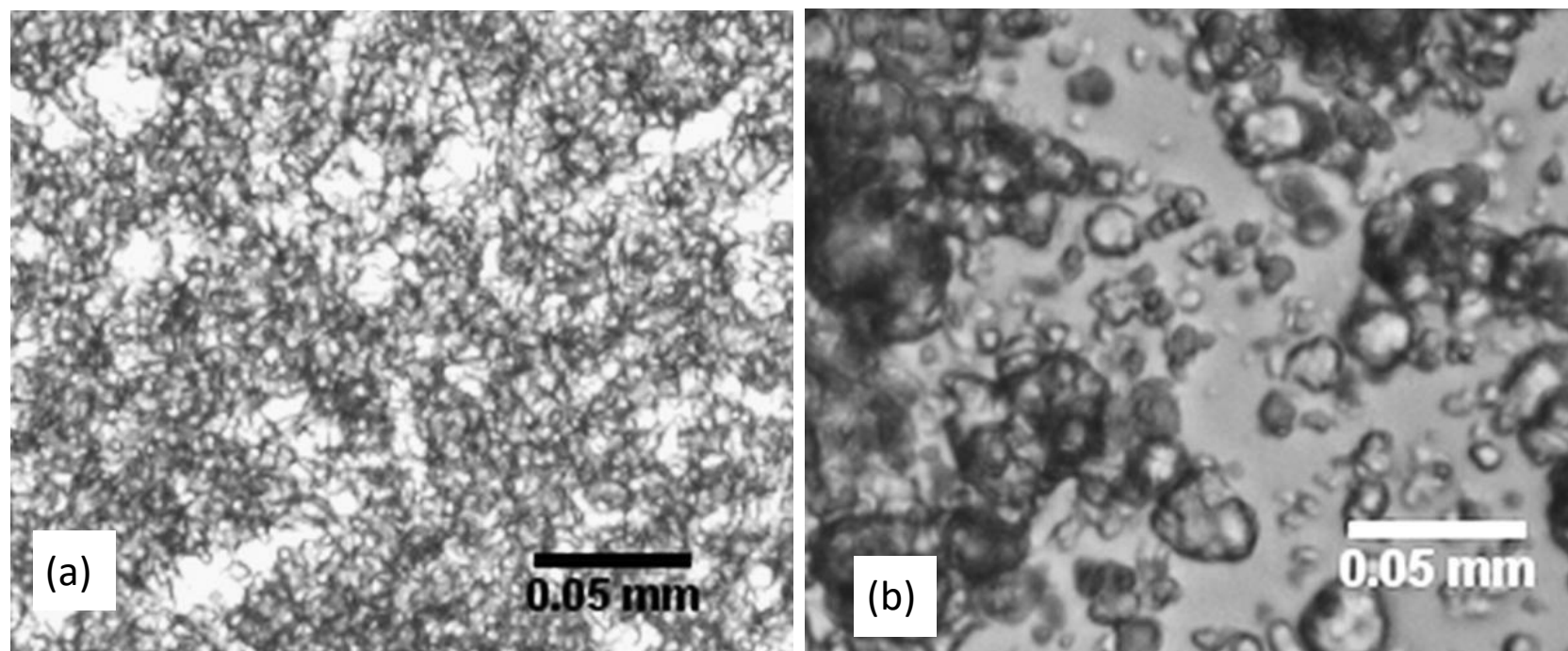


Fig. 1

Figure 2

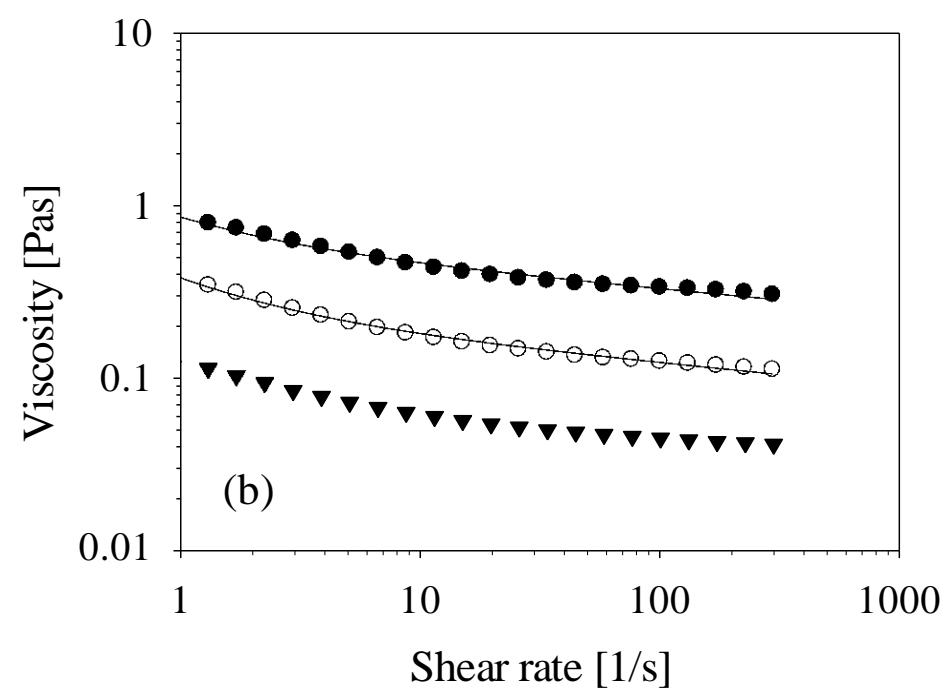
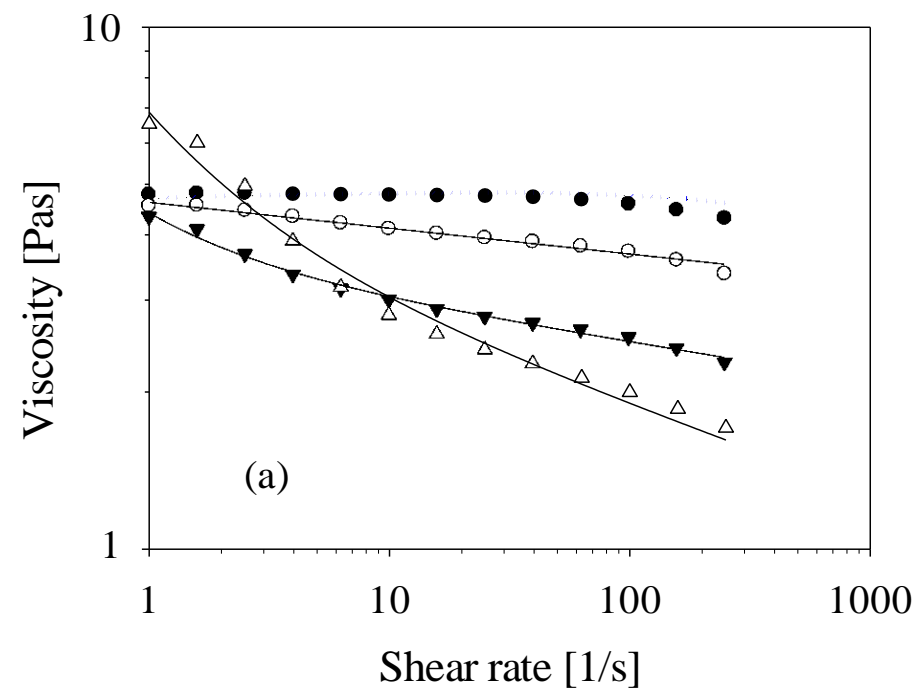


Figure 3

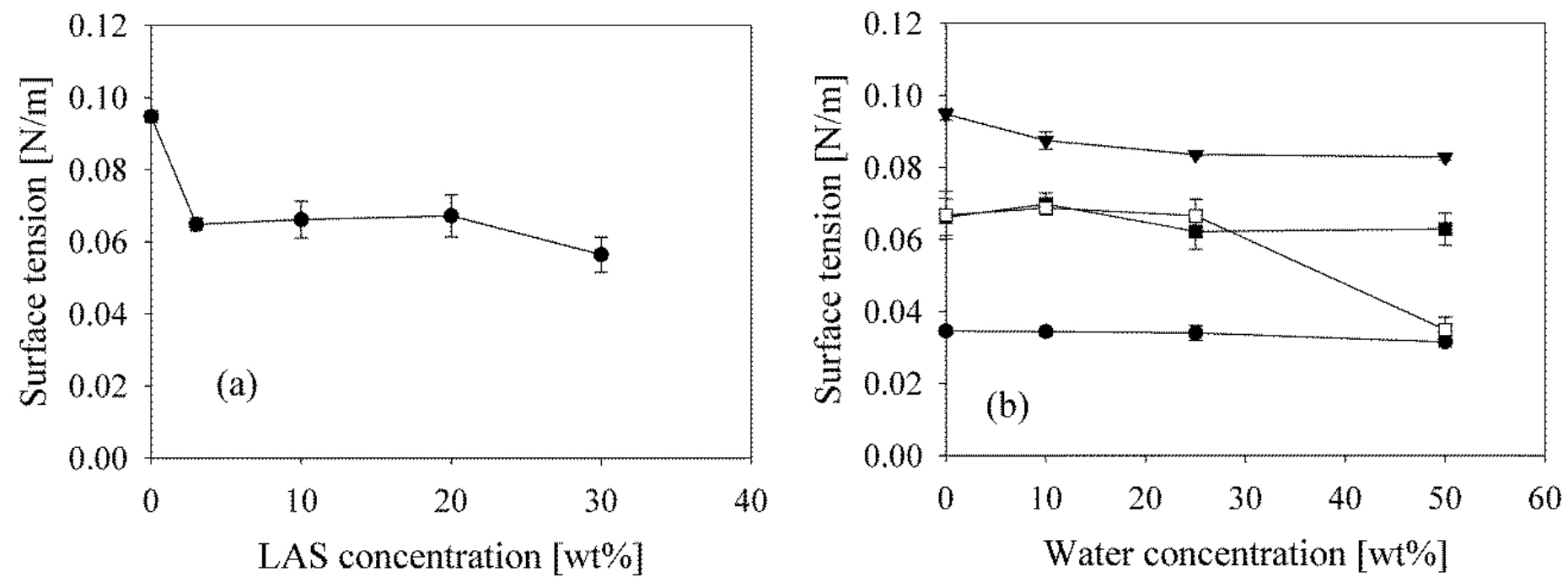


Fig. 3

Figure 4

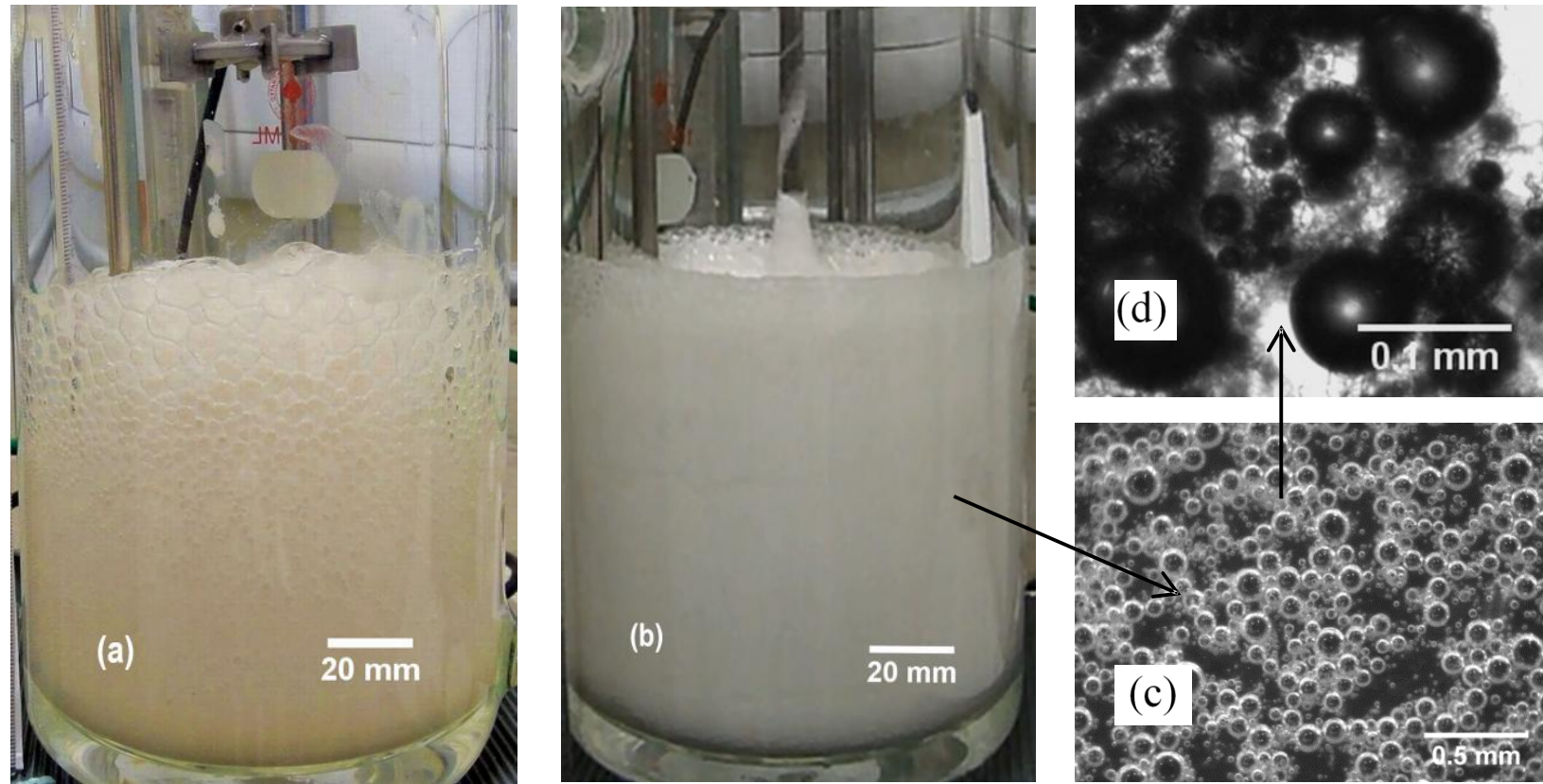


Fig. 4

Figure 5

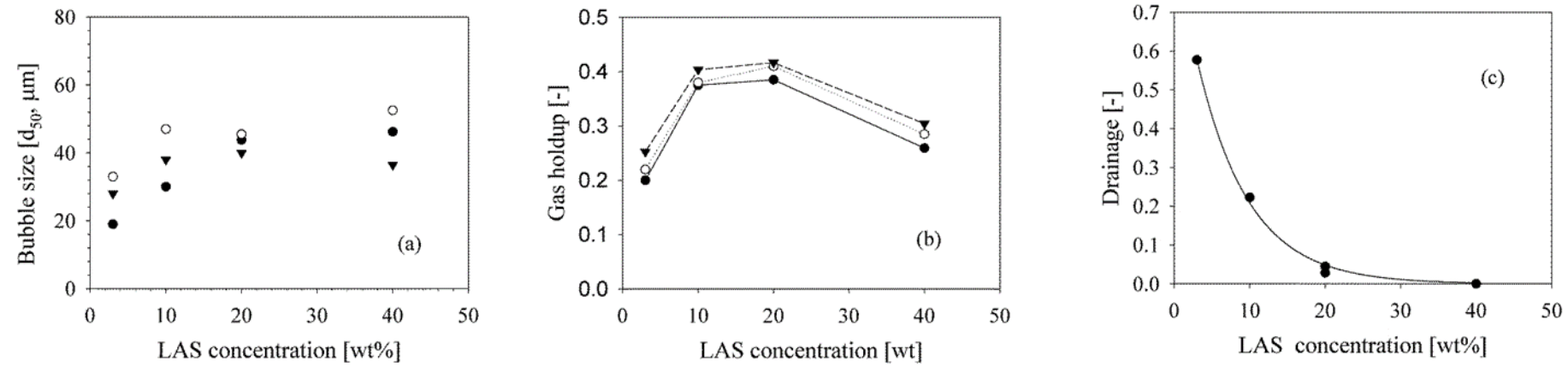


Fig. 5

Figure 6

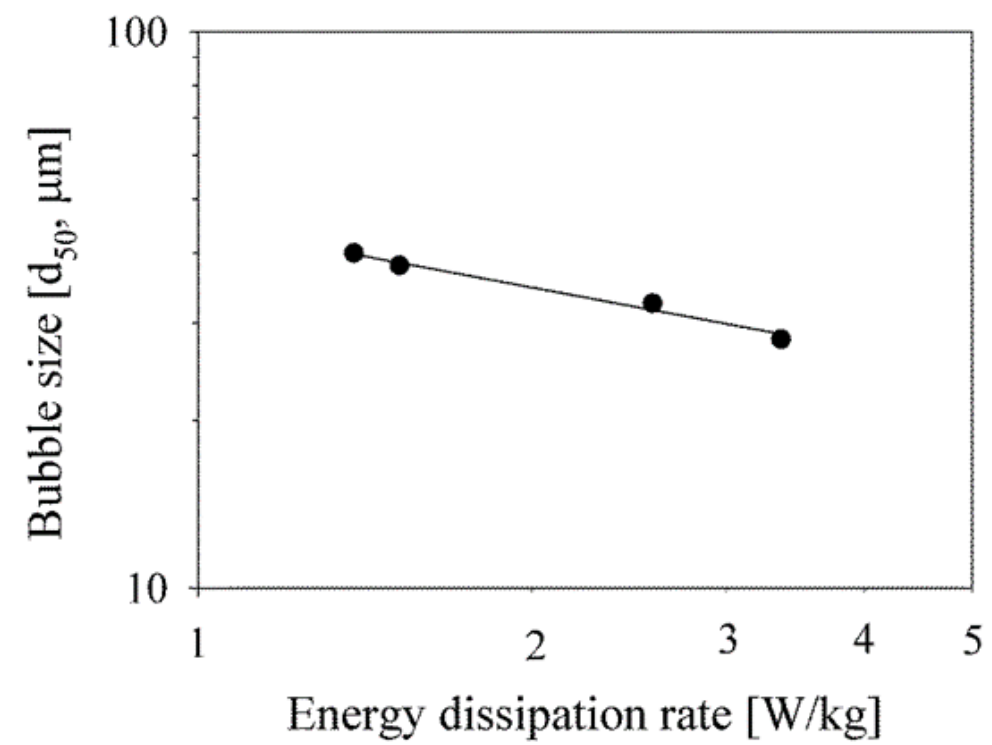


Fig. 6

Figure 7

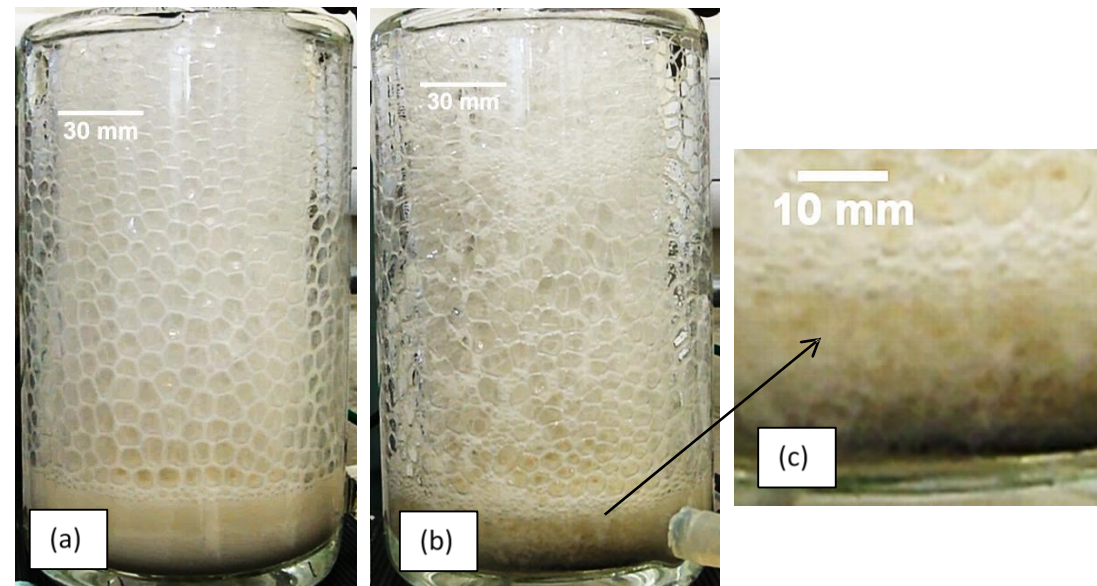


Fig. 7

Figure 8

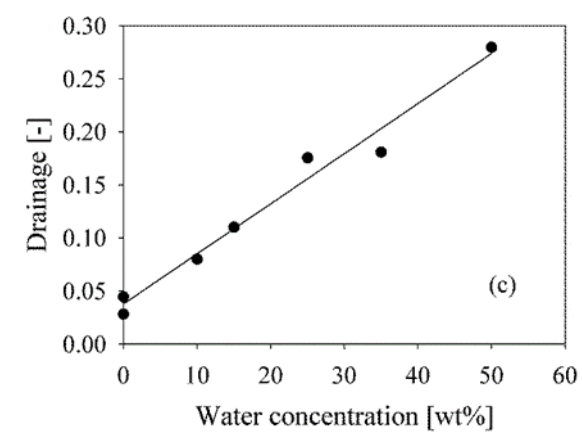
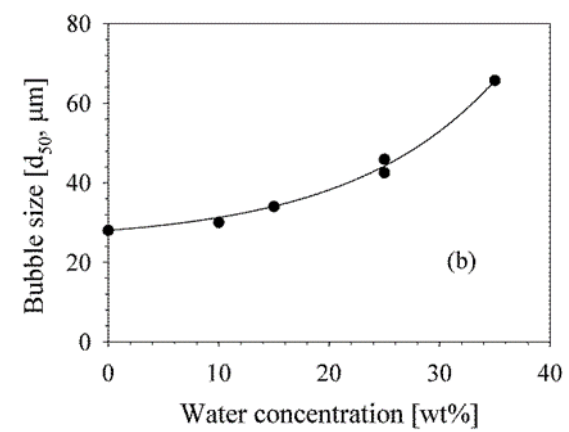
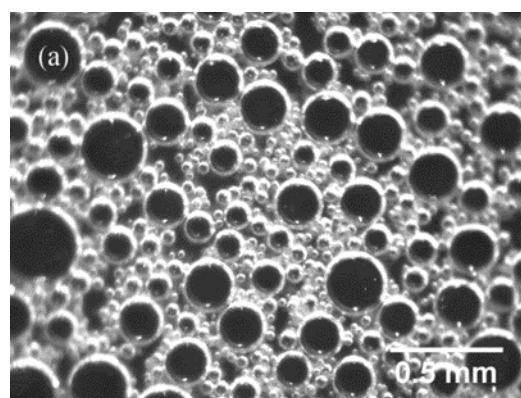


Fig. 8

Figure 9

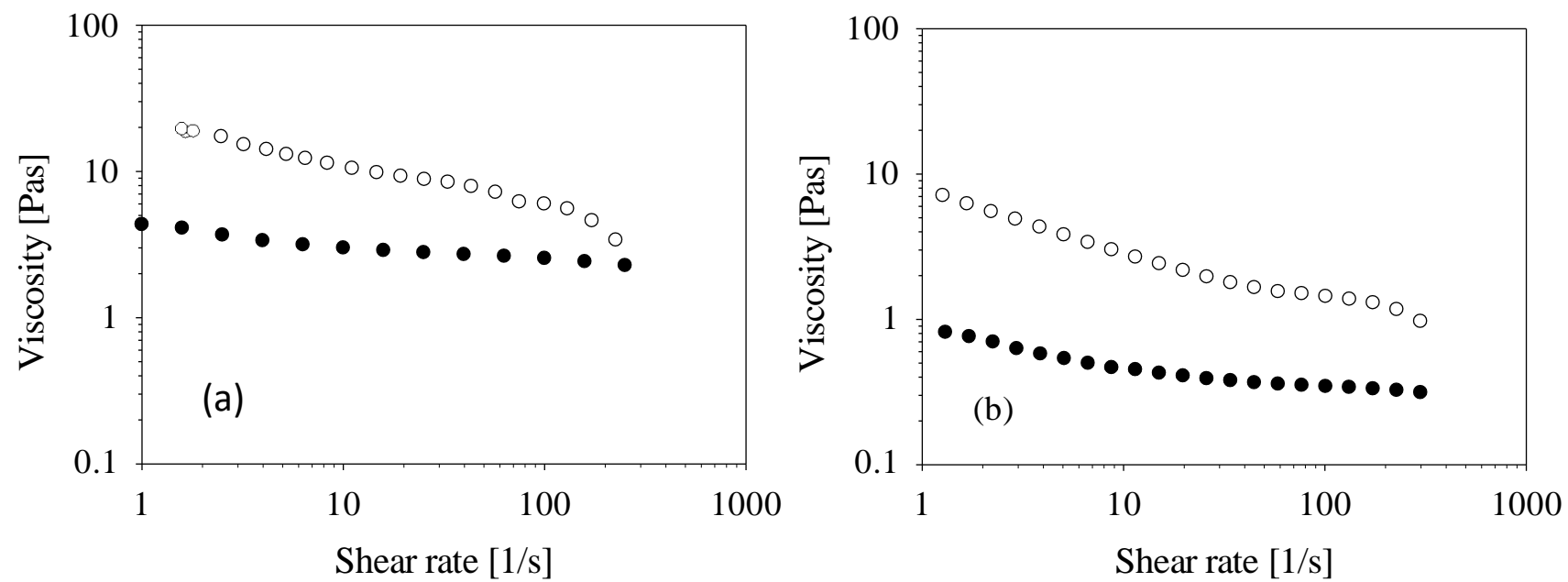


Fig. 9

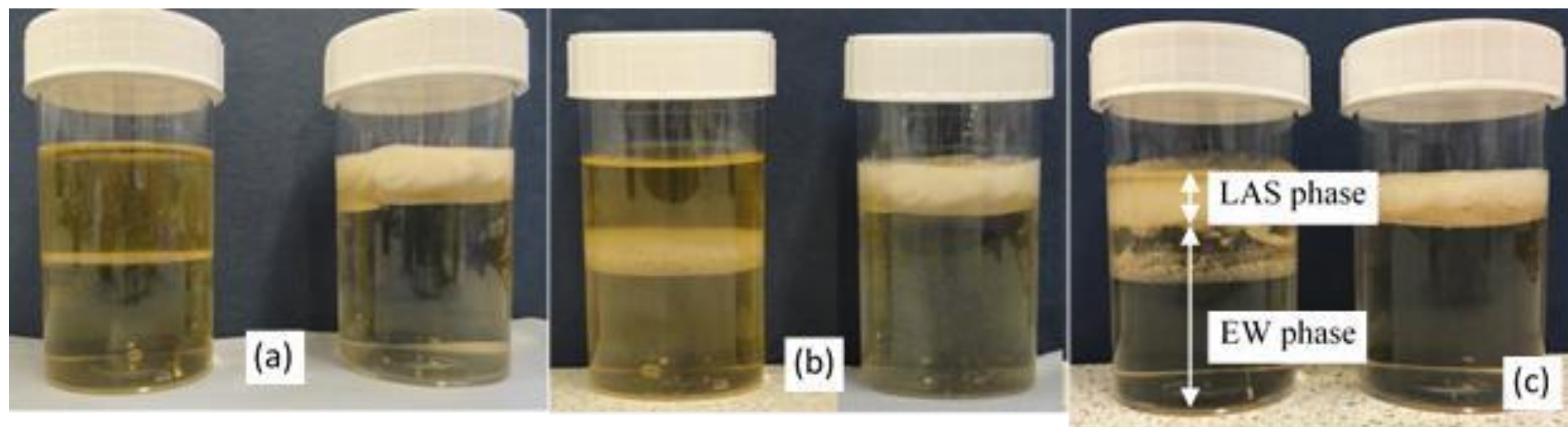


Fig. A1

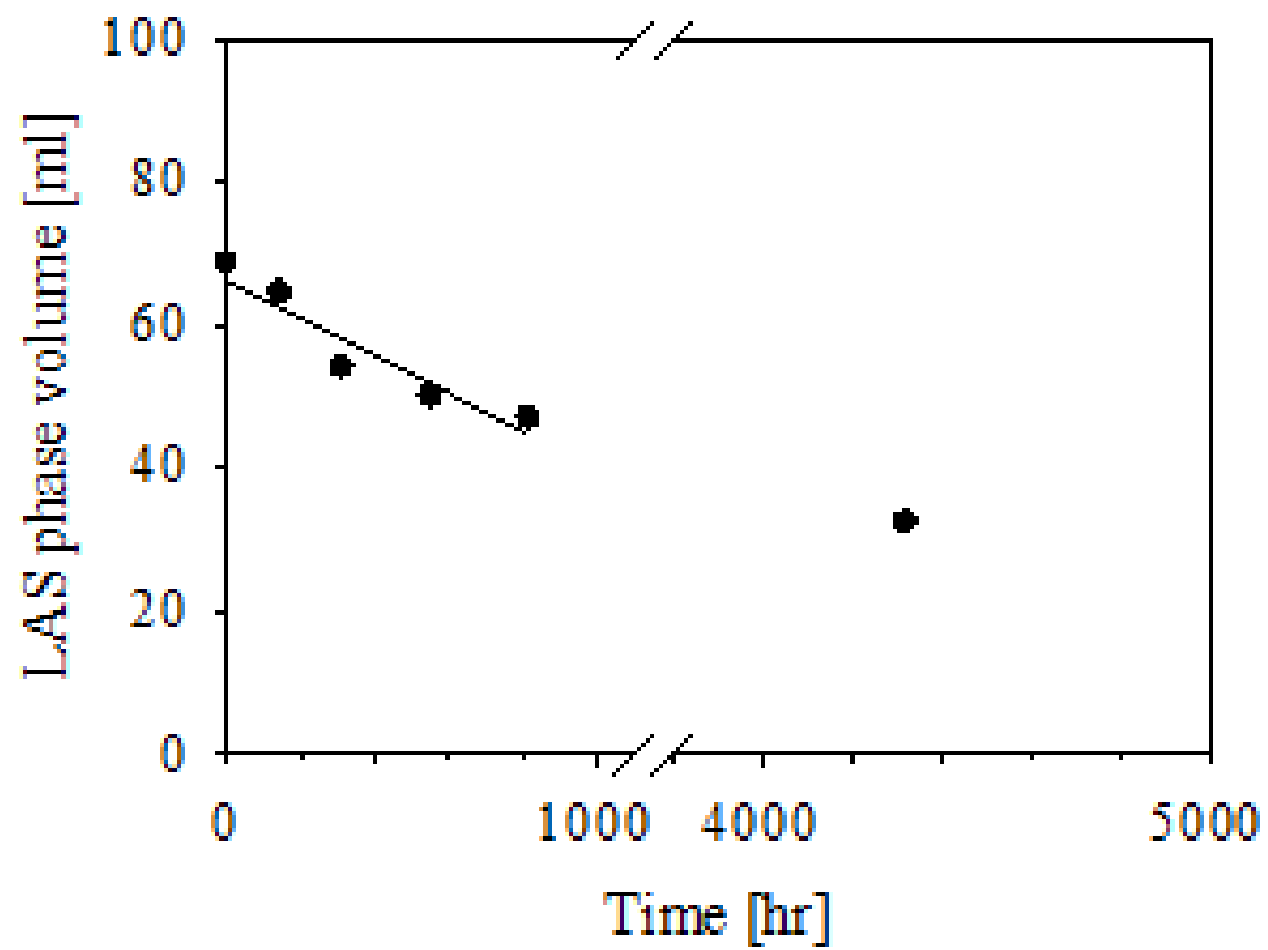


Fig. A2